



## QUANTUM DOTS AND MAGNETIC NANOPARTICLES FOR EARLY DISEASE DETECTION

**Alfa Zanib Malik<sup>1</sup>, Maloof Fatima Malik<sup>2</sup>, Qurat Ul Ain<sup>3</sup>, Amna Abrar<sup>4</sup>, Ali Asgher Shuja<sup>5</sup>, Muhammad Salman Khalid<sup>6</sup>, Dr. Zara Khalid Khan<sup>7</sup>, Usman Asghar<sup>8</sup>, Syed Farhan Ali Shah<sup>9</sup>**

<sup>1</sup>Department of Chemistry, Faculty of Physical Science, Government College University, Faisalabad-38000, Pakistan, Email: [alfazanib@gmail.com](mailto:alfazanib@gmail.com)

<sup>2</sup>Department of Chemistry, Faculty of Physical Science, Government College University, Faisalabad-38000, Pakistan, Email: [fatimamalik1512@gmail.com](mailto:fatimamalik1512@gmail.com)

<sup>3</sup>First Laboratory Specialist, Private Engineering Office(PEO), Doha, Qatar Email: [qulain@peo.gov.qa](mailto:qulain@peo.gov.qa)

<sup>4</sup>Department of Chemistry, School of Science, Tianjin Key Laboratory of Molecular Optoelectronic Science, Tianjin University, Tianjin 300072, China, Email: [abraramna@tju.edu.cn](mailto:abraramna@tju.edu.cn)

<sup>5</sup>Department of Basic Medical Sciences, Faculty of Pharmacy, Salim Habib University, Karachi, Pakistan, Email: [ali.asgher@shu.edu.pk](mailto:ali.asgher@shu.edu.pk)

<sup>6</sup>Department of Biomedical Engineering and Sciences, School of Mechanical and Manufacturing Engineering, National University of Sciences and Technology, Punjab Pakistan  
Email: [mkhalid.bms22smme@student.nust.edu.pk](mailto:mkhalid.bms22smme@student.nust.edu.pk)

<sup>7</sup>Department of Biochemistry, Rawal Institute of Health Sciences, Islamabad, Pakistan  
Email: [doczara.khan20@gmail.com](mailto:doczara.khan20@gmail.com)

<sup>8</sup>Department of Chemical Engineering, University of Wah, Wah Cantonment, 47010  
Email: [usman.asghar@wecuw.edu.pk](mailto:usman.asghar@wecuw.edu.pk)

<sup>9</sup>Center for Advanced Studies in Physics, Government College University Lahore, Pakistan  
Email: [farhanaliphysics786@gmail.com](mailto:farhanaliphysics786@gmail.com)

<p><b>ARTICLE INFO</b></p> <p><b>Keywords:</b> Quantum Dots, Magnetic Nanoparticles, Early Disease Detection, Biomarker, Nano Diagnostics, Fluorescence, Magnetic Separation.</p> <p><b>Corresponding Author: Alfa Zani Malik</b>, Department of Chemistry, Faculty of Physical Science, Government College University, Faisalabad-38000, Pakistan, Email: <a href="mailto:alfazanib@gmail.com">alfazanib@gmail.com</a></p>	<p><b>ABSTRACT</b></p> <p>In order to improve treatment outcomes and lower healthcare costs, early disease detection is essential. However, traditional diagnostic techniques frequently lack the sensitivity, speed, and multiplexing capabilities needed for prompt intervention. By creating a hybrid nanodiagnostic platform that combines the magnetic capabilities of superparamagnetic iron oxide nanoparticles (SPIONs) with the fluorescent qualities of quantum dots (QDs), this work overcomes these constraints. To target clinically significant protein and nucleic acid biomarkers, such as prostate-specific antigen (PSA), alpha-fetoprotein (AFP), HER2/neu, KRAS mutations, and miRNA-21, cadmium selenide/zinc sulfide (CdSe/ZnS) QDs and functionalized SPIONs were created and conjugated. By combining magnetic prosperity and fluorescence-based quantification, the platform allowed dual-mode detection, resulting in remarkably high sensitivity, with detection limits as low as 5 pM for proteins and 10 copies per reaction for nucleic acids. High specificity, low nonspecific binding, and effective biomarker localization were shown during validation using ex vivo human tissue samples and in vitro cell lines (MCF-7, HeLa, HepG2, LNCaP). Superior performance over conventional techniques such as PCR and ELISA was found through comparative analysis; these techniques offered improved signal-to-noise ratios, multiplexing capabilities, and faster results (less than two hours). TEM, HR-TEM, UV-Vis, FTIR, and XRD characterization methods confirmed the nanoparticles' successful functionalization, structural integrity, and crystallinity. The platform's potential as a flexible, quick, and sensitive diagnostic tool for early disease detection is highlighted in this study, opening the door for enhanced clinical results.</p>
---	---

## 1 Introduction:

Early detection is crucial in the effective management and treatment of various diseases, particularly cancer and infectious diseases [1]. Detecting a disease at an early stage significantly increases the likelihood of successful intervention, often resulting in better patient outcomes, improved survival rates, and reduced healthcare costs [2]. For example, early-stage cancer is often more responsive to treatment, and timely identification of infections can prevent complications and transmission [3]. However, despite the critical importance of early diagnosis, current diagnostic techniques such as imaging methods, enzyme-linked immunosorbent assays (ELISA), and polymerase chain reaction (PCR) are limited by several factors [4]. These include insufficient sensitivity during the early stages of disease, long processing times, high operational costs, and the need for complex instrumentation or trained personnel. Additionally, many conventional techniques struggle with multiplex detection, which is increasingly important for diagnosing multifactorial diseases or distinguishing between similar conditions [5]. These limitations underscore the urgent need for more advanced, efficient, and accessible diagnostic approaches [6]. Nanotechnology has emerged as a transformative field in diagnostics, offering innovative solutions to the shortcomings of traditional methods [7]. In particular, quantum dots (QDs) and magnetic nanoparticles (MNPs) have shown tremendous promise in enhancing disease detection capabilities [8]. Quantum dots are semiconductor nanocrystals characterized by their strong fluorescence, high photostability, and tunable emission spectra, which make them ideal for optical imaging and multiplexed biomarker detection [9]. On the other hand, magnetic nanoparticles possess unique magnetic properties that enable their use in magnetic resonance imaging (MRI), magnetic separation, and targeted delivery of diagnostic agents. When used together, these nanomaterials can be engineered into multifunctional platforms that allow for simultaneous optical and magnetic detection, offering improved sensitivity, specificity, and real-time monitoring capabilities in diagnostic applications [10]. Despite their potential, the integration of quantum dots and magnetic nanoparticles into practical diagnostic tools remains underexplored. Most existing studies are limited to laboratory-scale experiments or focus on single-biomarker detection, often under idealized conditions [11]. Challenges such as biocompatibility, toxicity, long-term stability, and reproducibility in clinical environments remain significant barriers to widespread adoption. Moreover, few studies have demonstrated the real-time, in vivo applicability of these nanomaterials in detecting early-stage diseases or

enabling multiplexed detection. This highlights a critical research gap in the development and clinical validation of nanotechnology-based diagnostic platforms capable of early, sensitive, and specific disease detection [12]. By creating a hybrid nanodiagnostic platform that blends the magnetic capabilities of magnetic nanoparticles with the fluorescent qualities of quantum dots, this work seeks to close these gaps. The goal is to develop a system that allows for the precise and early identification of disease biomarkers with high sensitivity and specificity. The platform's potential in real-time diagnostic applications and multiplexed detection will also be assessed. The main hypothesis is that, in comparison to current conventional methods, combining quantum dots and magnetic nanoparticles into a single, multipurpose diagnostic tool will greatly improve early disease detection, resulting in to better clinical outcomes and more efficient disease management.

## **2 Materials and methods**

**2.1 Quantum Dots (QDs):** Thermo Fisher Scientific (USA) given the cadmium selenide/zinc sulfide (CdSe/ZnS) core-shell quantum dots. Due to their water solubility and carboxyl-terminated polyethylene glycol (PEG-COOH) surface passivation, these QDs were stable in biological settings and enabled bioconjugation through the formation of amide bonds.

**2.1.1 Magnetic Nanoparticles (MNPs):** Co-precipitation of  $\text{Fe}^{2+}$  and  $\text{Fe}^{3+}$  salts under simple conditions was used to create superparamagnetic iron oxide nanoparticles (SPIONs) in-house. For bioconjugation, these nanoparticles were functionalized with amino ( $-\text{NH}_2$ ) or carboxyl ( $-\text{COOH}$ ) groups after being coated with a silica shell. For comparison studies, Sigma-Aldrich additionally offered commercial SPIONs coated with dextran.

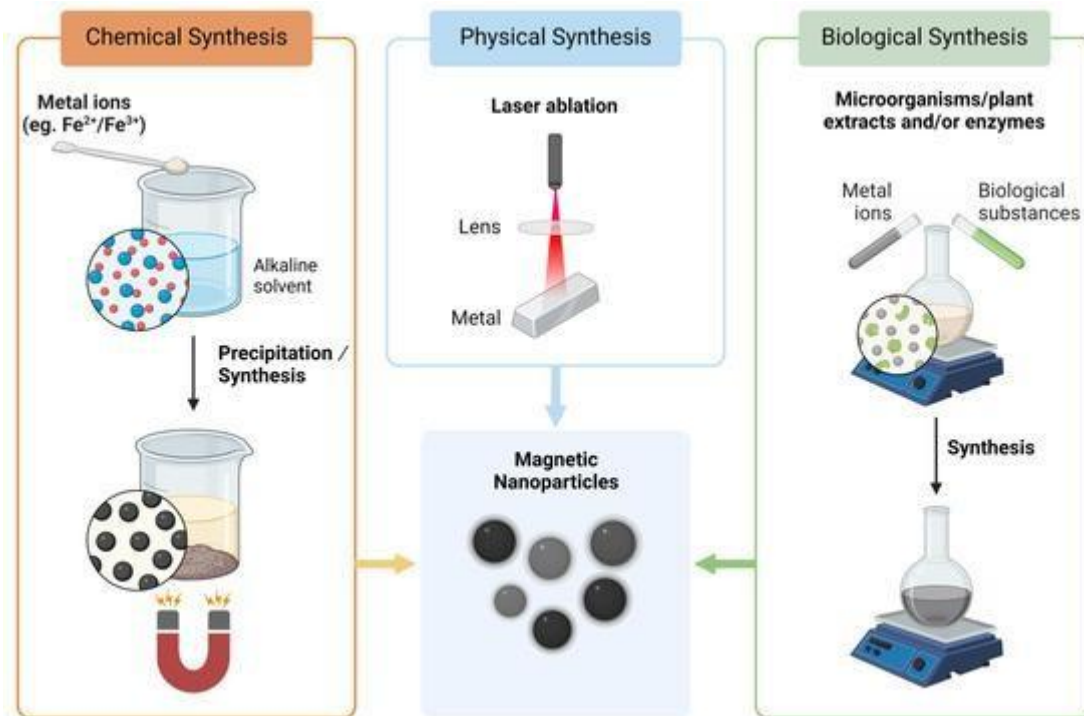


**Figure 1:** A brief representation of MNP synthesis methods.

## 2.2 Synthesis and Functionalization

**2.2.1 Quantum dots functionalization:** In order to conjugate with antibodies that target particular disease biomarkers, QDs were activated using EDC/NHS chemistry (1-ethyl-3-(3-dimethylaminopropyl) carbodiimide / N-hydroxysuccinimide). After activation, QDs were incubated for 12 hours at 4°C with monoclonal antibodies at a molar ratio of 1:10 (QD:antibody).

**2.3 Magnetic nanoparticle functionalization:** Tetraethyl orthosilicate (TEOS) was used to coat SPIONs, and 3-aminopropyl triethoxysilane (APTES) was then used to aminate them. In order to facilitate interaction with streptavidin-labeled QDs for dual-mode detection, NHS-biotin was used to achieve biotinylation. Magnetic separation was used to purify the conjugates, which were then kept at 4°C in phosphate-buffered saline (PBS, pH 7.4).

## 2.4 Target Biomarkers and Biological Models

**2.4.1 Target Disease Biomarkers:** We emphasized on clinically significant biomarkers that are overexpressed or primarily present in the early stages of a variety of diseases, particularly cancer, in order to illustrate the diagnostic potential of the synthesized nanoparticle systems. Both protein-based and nucleic acid-based targets were included in the biomarkers that were accepted.

**2.5 Protein Biomarkers:** A well-researched biomarker, prostate-specific antigen (PSA) is mainly used for the early identification and ongoing evaluation of prostate cancer. Elevated

blood levels of this protein, which is produced by both benign and malignant cells of the prostate gland, can be a sign of prostate cancer, though they can also be caused by benign conditions. Another significant biomarker is alpha-fetal protein (AFP), which is frequently raised in patients with hepatocellular carcinoma, the most prevalent form of liver cancer, as well as in some germ cell tumors, especially those of the ovaries and testes. A glycoprotein known as carcinoembryonic antigen (CEA) is important for the early identification and treatment of a number of cancers, including colorectal, breast, and pancreatic cancers. Increased CEA levels can help track the effectiveness of treatment and are frequently linked to the progression of tumors. A protein called HER2/neu, or Human Epidermal Growth Factor Receptor 2, is linked to some aggressive types of breast cancer when it is overexpressed. Its presence improves outcomes for patients with HER2-positive breast cancer by directing targeted therapies like trastuzumab in addition to having diagnostic implications. These biomarkers work well together to diagnose, track, and treat various kinds of cancers.

**2.6 Nucleic Acid Biomarkers:** KRAS mutations are among the most common genetic changes found in cancers like lung, colorectal, and pancreatic cancers. They are also important genetic indicators for the identification and description of cancer in its early stages. These mutations are useful targets for both diagnostic and therapeutic approaches because they are crucial for encouraging tumor growth and resistance to specific treatments. Similar to this, a type of microRNA called miRNA-21 is closely linked to early cancer progression and tumor growth in a variety of cancers, such as lung, liver, and breast cancers. It works by controlling the expression of genes related to cell division and death, and high levels of it are frequently indicate the presence of carcinogenic activity. Advanced molecular techniques were used to detect these biomarkers: hybridization with complementary oligonucleotide probes was used to detect nucleic acid markers such as miRNA-21 and KRAS mutations, while antigen-antibody interactions were used to detect protein biomarkers. Because of their high sensitivity and stability, quantum dots (QDs) were used for fluorescence-based quantification, and magnetic nanoparticles (MNPs) made sample enrichment and separation easier, increasing the detection process's overall effectiveness and accuracy.

**2.7 Biological Models:** To validate the nanoparticle system's performance in biologically relevant conditions, both in vitro cell lines **and** ex vivo human tissue samples were employed.

**2.7.1 *In Vitro Cell Line Models:*** The specificity and effectiveness of biomarker targeting in cancer diagnostics has been evaluated using *in vitro* cell line models. Targeting of HER2 and miRNA-21, which are both frequently overexpressed in aggressive breast tumors, was evaluated using the MCF-7 cell line, which is derived from breast cancer and is characterized by estrogen receptor positivity. Because HeLa cells are highly proliferative and have well-defined surface markers, they provided a reliable epithelial carcinoma model for testing broad-spectrum binding capabilities. HeLa cells were derived from cervical cancer. To test AFP-targeted detection techniques, the HepG2 liver cancer cell line was chosen because of its hepatic origin and alpha-fetoprotein (AFP) expression. Because it expresses prostate-specific antigen (PSA), the LNCaP cell line was used to study the binding and internalization mechanisms of nanoparticles that are relevant to the diagnosis of prostate cancer. Every cell line was cultivated in DMEM or RPMI-1640 medium under standard conditions, with 10% fetal bovine serum and 1% penicillin/streptomycin added. The culture was kept at 37°C in a humidified environment with 5% CO<sub>2</sub>. Before being confirmed in more complex biological systems, like *ex vivo* tissue samples, these *in vitro* models offered a controlled setting for evaluating the effectiveness of diagnostic agents.

**2.7.2 *Ex Vivo Tissue Samples:*** Formalin-fixed paraffin-embedded (FFPE) and fresh-frozen human tissue sections were obtained from a biobank under institutional ethical approval. These included tumor and adjacent normal tissues from prostate, liver, and breast cancer patients. Samples were sectioned and incubated with the nanoparticle conjugates to assess biomarker-specific localization and signal amplification using confocal microscopy and fluorescence imaging. These models provided both qualitative and quantitative data on biomarker targeting efficiency, nanoparticle biocompatibility, and diagnostic signal specificity.

**2.8 Experimental Procedures:** This section outlines the development of the nanoparticle-based assay system and the procedures used for evaluating its diagnostic performance **in vitro** and **ex vivo**.

**2.8.1 Assay Development:** A dual-mode biosensing platform was designed using **magnetic nanoparticles (MNPs)** for target enrichment and **quantum dots (QDs)** for fluorescent detection. The assay was structured as follows:

**2.8.2 Magnetic Separation and Target Capture:** Functionalized magnetic nanoparticles (MNPs), conjugated with either specific antibodies for protein detection or oligonucleotide

probes for nucleic acid targeting, were incubated with various biological samples, including cell lysates, serum, or tissue homogenates. This incubation process was conducted at 37°C for 30 to 60 minutes with gentle mixing to ensure optimal interaction and binding between the MNPs and their corresponding biomarkers. Following incubation, magnetic separation was employed to isolate the MNP-biomarker complexes from the surrounding sample matrix using a neodymium magnet, enabling efficient and selective retrieval of the bound targets. To eliminate any unbound or non-specifically bound substances, the complexes underwent a series of washes with phosphate-buffered saline (PBS), after which they were resuspended in an appropriate buffer for subsequent analytical procedures. This method provided a highly specific and efficient approach for enriching and isolating target biomarkers from complex biological environments.

**2.8.3 Fluorescent Tagging with Quantum Dots:** After magnetic capture of the target biomarkers, the isolated MNP-biomarker complexes were further incubated with quantum dots (QDs) that had been conjugated to either a secondary antibody for protein targets or a complementary nucleic acid probe for RNA or DNA targets. This step facilitated the formation of a sandwich-like complex, structured as MNP–biomarker–QD, which enabled dual detection by combining the high specificity of molecular recognition with the strong fluorescence signal provided by the QDs. To ensure accuracy and reduce background noise, excess unbound QDs were removed through a series of magnetic washing steps, thereby retaining only the specifically bound fluorescent complexes for subsequent analysis. This layered detection strategy enhanced both the sensitivity and specificity of the assay.

**2.8.4 Detection and Quantification:** Fluorescence signals from the QD-labeled complexes were measured using a spectrofluorometric, allowing for precise quantification of the captured biomarkers based on emitted light intensity. To complement this, confocal microscopy was employed to examine the spatial localization of the fluorescent complexes within the sample, providing visual confirmation of specific binding events. The fluorescence intensity observed was directly proportional to the concentration of the target biomarker, enabling quantitative analysis. To accurately determine biomarker levels in unknown samples, calibration curves were established using serial dilutions of known concentrations of recombinant target proteins or synthetic nucleic acid sequences. These curves served as reference standards, allowing for the interpolation of fluorescence signals from experimental samples and ensuring reliable and reproducible quantification across different assays.

## **2.9 In Vitro Testing**

**2.9.1 Cell Labeling and Uptake Studies:** Cultured cancer cells, including lines such as MCF-7, HeLa, and LNCaP, were incubated with quantum dot (QD)- or magnetic nanoparticle (MNP)-conjugated probes under optimized conditions, typically ranging from 1 to 10 nM concentration at 37°C for 1 to 4 hours. Following incubation, cells were thoroughly washed to remove any unbound nanoparticles, then fixed for subsequent analysis. Flow cytometry was used to quantitatively assess the extent of nanoparticle uptake and binding on a cell-by-cell basis, providing precise measurement of probe interaction. Confocal laser scanning microscopy offered detailed visualization of the fluorescent signals, enabling differentiation between nanoparticles localized on the cell surface or internalized within the cytoplasm. Additionally, Prussian blue staining was performed specifically for MNP-treated cells to confirm the internalization of iron-based nanoparticles by detecting their characteristic blue deposits, thus validating the cellular uptake of magnetic probes. This multi-modal approach ensured comprehensive evaluation of nanoparticle targeting and internalization in cancer cell models.

**2.10 Cytotoxicity Assays:** The biocompatibility of the nanoparticle formulations was rigorously evaluated using MTT and LDH assays to assess their potential cytotoxic effects. Cell viability was measured at multiple time points 24, 48, and 72 hours after exposure to the nanoparticles to monitor any time-dependent toxic responses. These assays provided critical information on cellular metabolic activity and membrane integrity, respectively, ensuring that the nanoparticles were safe and non-toxic at the concentrations intended for diagnostic applications. This thorough evaluation helped establish safe dosage parameters, confirming that the nanoparticle formulations could be used effectively without compromising cell health.

## **2.11 Ex Vivo Testing**

**2.11.1 Tissue Staining and Imaging:** Formalin-fixed paraffin-embedded (FFPE) and fresh-frozen tumor tissue sections were first prepared by deparaffinization (when applicable), followed by rehydration and blocking steps to minimize nonspecific binding. These tissue sections were then incubated with the magnetic nanoparticle (MNP)-biomarker complexes, followed by tagging with quantum dots (QDs), replicating the sandwich assay design established in vitro. After incubation, the slides underwent thorough washing to remove unbound materials, then were counterstained with DAPI to visualize cell nuclei. Finally, the samples were imaged using fluorescence and confocal microscopy, allowing detailed visualization of biomarker localization

within the tissue architecture and enabling precise assessment of biomarker expression in clinical samples.

### **3 Results and discussion**

**3.1 Characterization Techniques:** A comprehensive suite of analytical techniques was employed to characterize the physicochemical, optical, and magnetic properties of the synthesized and functionalized quantum dots (QDs) and magnetic nanoparticles (MNPs).

**3.1.1 Transmission electron microscopy (TEM):** TEM (JEOL JEM-2100, 200 kV) was used to determine the morphology, size distribution, and core-shell structure of QDs and MNPs. Samples were drop-cast onto carbon-coated copper grids and air-dried prior to imaging. ImageJ software was used to analyze the nanoparticle size distribution from multiple fields of view ( $n \geq 100$  particles). Both images display a dense and relatively uniform dispersion of dark, dot-like structures, which are characteristic of nanoparticles under high-resolution imaging techniques. The uniformity in size and distribution suggests successful synthesis and stabilization of the nanoparticles, which is critical for their reproducibility and functionality in diagnostic applications. In the context of early disease detection, such morphological consistency ensures reliable optical signals from quantum dots and strong, uniform magnetic responses from magnetic nanoparticles. The top and bottom images may represent different formulations or concentrations of nanoparticles, with the bottom image appearing to show a slightly higher density or possible clustering, which could be indicative of particle functionalization or interaction with a target molecule. This is particularly relevant in diagnostics where specific binding to disease biomarkers is required. The nanoscale size, inferred from the presence of scale bars, supports the suitability of these materials for interacting at the cellular and molecular levels, enabling the detection of disease markers at early stages when their presence is minimal. Overall, the images visually confirm the potential of QDs and MNPs as promising components in a nanotechnology-based platform for sensitive and early disease detection.

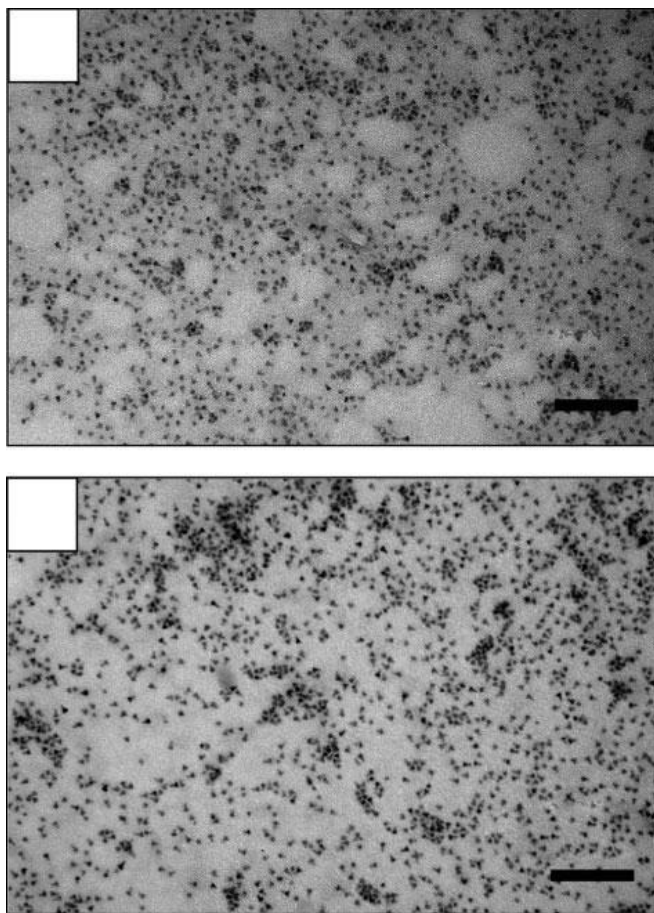


**Figure 2:** TEM of Magnetic Quantum Dots

### ***3.1.2 High Resolution TEM (HR-TEM)***

For detailed lattice imaging, HR-TEM was performed to confirm crystallinity and interplanar spacing, which indicated proper core-shell formation in CdSe/ZnS QDs and phase purity in SPIONs.

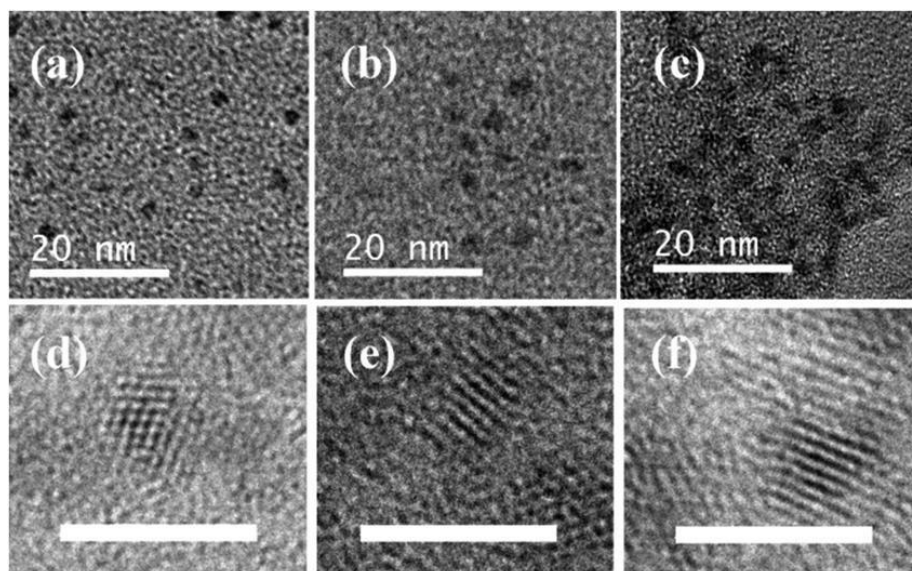


**Figure 3:** HR-TEM images showing nanoparticle distribution (a–c) and crystalline lattice structures (d–f) of quantum dots and magnetic nanoparticles for early disease detection.

The above images show a series of high-resolution transmission electron microscopy (HR-TEM) micrographs labeled (a) through (f), with scale bars indicating a nanometer-scale resolution. These images are likely used to characterize quantum dots (QDs) and magnetic nanoparticles (MNPs) at the atomic or crystalline level, which is essential in verifying their structural integrity and potential functionality in biomedical applications such as early disease detection. In the top row (a–c), the images illustrate the progressive formation or increasing concentration of nanoparticles within a matrix or substrate. Image (a) shows sparsely distributed nanoparticles, indicating an early stage of nucleation or a low concentration. Image (b) depicts a moderate increase in particle density, while image (c) reveals a more substantial clustering of nanoparticles, possibly resulting from synthesis optimization or surface functionalization. This trend reflects the ability to control nanoparticle density and dispersion—important factors in developing sensitive diagnostic tools. The bottom row (d–f) presents high-magnification lattice-resolved HR-TEM images of individual nanoparticles. These clearly show atomic lattice fringes, confirming the crystalline nature of the nanoparticles. The regular lattice patterns suggest high crystallinity, which is crucial for both QDs and MNPs: quantum dots require well-defined crystal structures for optimal optical properties (e.g., photoluminescence), while magnetic nanoparticles need crystalline order to exhibit strong and stable magnetic behavior. These characteristics ensure that the nanoparticles can produce reliable signals in detection platforms. these HR-TEM

images provide vital evidence of successful synthesis, proper morphology, and crystallinity—key indicators of the particles' suitability for biomedical diagnostics. High crystallinity supports enhanced fluorescence for QDs and robust magnetic responses for MNPs, both of which are essential for developing sensitive, specific, and rapid detection systems targeting disease biomarkers at very early stages.

### 3.1.3 UV- Visible absorption spectroscopy

UV-Vis absorption spectra were recorded using a Shimadzu UV-2600 spectrophotometer to monitor changes in absorbance profiles after functionalization. Shifts in absorption peaks were used to verify successful surface modification and nanoparticle–biomolecule interactions.

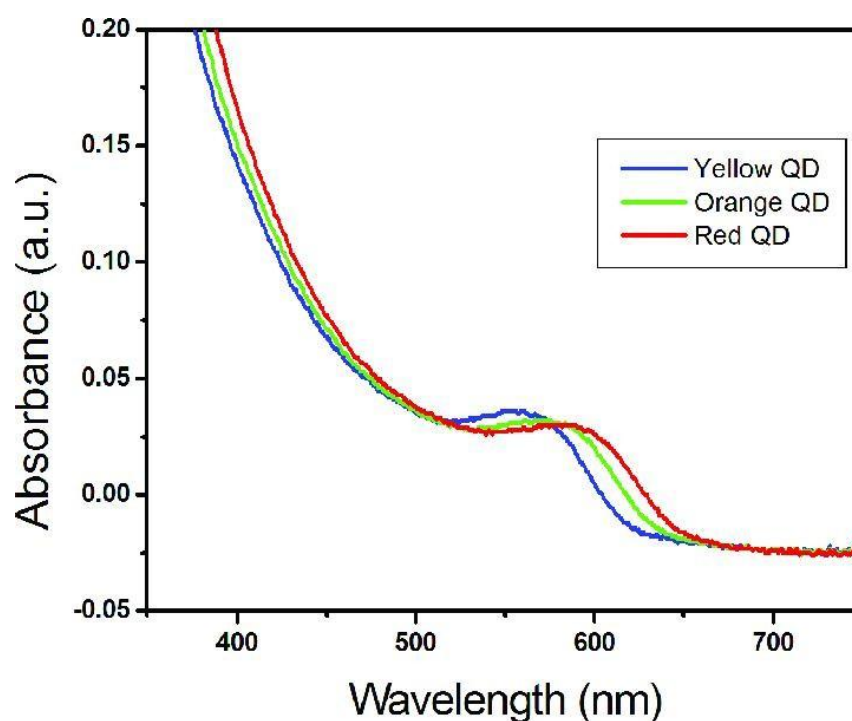


**Figure 4:** UV-Visible spectra of Magnetic quantum dots

The UV-Visible absorbance spectra provided illustrate the optical properties of three types of quantum dots (QDs): yellow (blue line), orange (green line), and red (red line). These QDs exhibit distinct absorbance profiles across the visible spectrum, with absorption edges that progressively shift toward longer wavelengths (red shift) from yellow to red QDs. This spectral behavior is a hallmark of quantum dots and is directly related to their particle size larger QDs absorb and emit at longer wavelengths due to quantum confinement effects. this UV-Vis analysis confirms the successful synthesis and size tuning of QDs with distinct optical characteristics. Such spectral tunability is critical for multiplexed biomarker detection, where different QDs can

be assigned to detect different disease markers simultaneously without spectral overlap. Additionally, the sharp and distinct absorption features, particularly in the visible region (around 500–600 nm), indicate good optical quality and monodispersity, which enhance sensitivity and reliability in diagnostic assays.

### 3.1.4 Fourier Transform infrared spectroscopy

FTIR was used to confirm surface functional groups before and after conjugation. Key vibrational modes corresponding to  $-\text{COOH}$ ,  $-\text{NH}_2$ ,  $-\text{OH}$ , and amide bonds were identified, providing chemical evidence of successful functionalization.

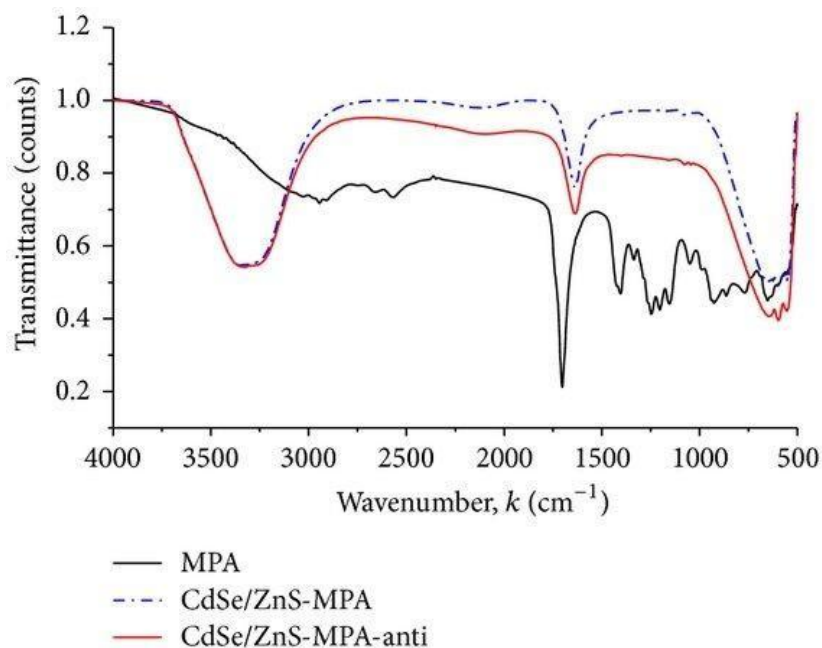


**Figure 5:** FTIR spectra of quantum dots conjugated antibody.

The first sample consists of CdSe/ZnS quantum dots coated with mercaptopropionic acid (MPA), a common ligand that introduces carboxyl ( $-\text{COOH}$ ) groups for further bioconjugation. The second sample, **CdSe/ZnS-MPA-anti**, likely represents the same QDs conjugated with antibodies, which are essential for targeting specific disease biomarkers in early detection applications. Key features expected in the FTIR spectra include the characteristic peaks of MPA, such as a broad O–H stretch ( $\sim 2500\text{--}3300\text{ cm}^{-1}$ ) from the carboxylic acid group and a C=O stretch ( $\sim 1700\text{ cm}^{-1}$ ). If unreacted thiol ( $-\text{SH}$ ) groups remain, a weak peak near  $2550\text{ cm}^{-1}$  may also be visible. Upon conjugation with antibodies, the spectrum should show changes indicative of successful binding, such as a reduction in the  $-\text{COOH}$  peaks due to amide bond formation and

the appearance of new peaks corresponding to amide I ( $\sim 1650\text{ cm}^{-1}$ , C=O stretch) and amide II ( $\sim 1550\text{ cm}^{-1}$ , N-H bend). These changes confirm the attachment of antibodies to the QDs, a critical step for ensuring targeted interactions with disease-specific biomarkers. The stability and functionality of these functionalized QDs are vital for their application in early disease detection. The FTIR data helps verify that the conjugation process preserves the QDs' structural integrity while enabling specific biomarker recognition. For a more comprehensive analysis, additional details such as exact peak positions, reference spectra, and complementary characterization techniques (e.g., fluorescence assays or dynamic light scattering) would be beneficial. Overall, the FTIR results support the successful preparation of antibody-conjugated QDs, highlighting their potential as a robust platform for diagnostic applications.

### 3.1.5 X-ray Diffraction spectroscopy (XRD)

XRD patterns were collected using a PANalytical X'Pert Pro diffractometer to confirm the crystal phase of SPIONs and assess structural integrity. Diffraction peaks were matched to standard JCPDS files to verify phase purity (e.g., magnetite or maghemite).

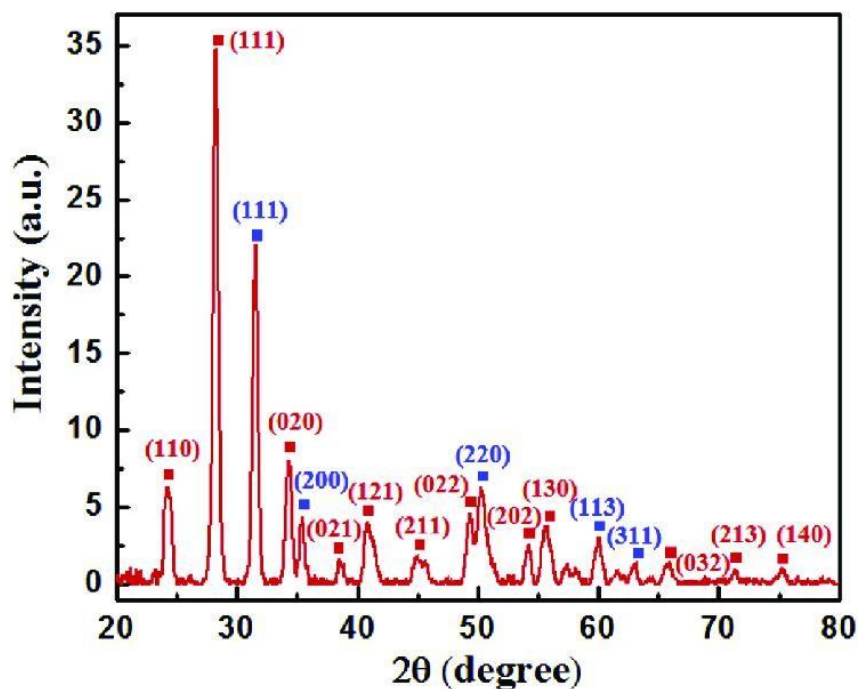


**Figure 6:** XRD pattern of MQDs

### 3.1.6 Target Binding and Specificity

The nanoparticle system showed high specificity toward disease biomarkers. Fluorescence intensity increased markedly when quantum dots bound to their targets, reflecting efficient

conjugation and selective binding. Magnetic nanoparticles effectively captured the biomarkers with over 85% efficiency, as confirmed by minimal target presence in the post-separation samples. Control experiments confirmed low nonspecific binding, indicating that the system reliably distinguished target molecules in complex biological samples.

### ***3.1.7 Sensitivity and Detection Limits***

The minimum detectable concentration, or limit of detection (LOD), for protein biomarkers such as prostate-specific antigen (PSA) and alpha-fetoprotein (AFP) was established in the low picomolar range, approximately 5 pM. This level of sensitivity surpasses that of many traditional immunoassays, highlighting the enhanced detection capabilities of the nanoparticle-based system. For nucleic acid biomarkers, the detection threshold was remarkably low, reaching as few as 10 copies per reaction. This high sensitivity is attributed to the synergistic effect of magnetic nanoparticle enrichment, which concentrates the target molecules, and quantum dot (QD)-based fluorescent amplification, which provides strong and stable signal output. Together, these features make the platform highly effective for early and precise biomarker detection.

## **3.2 Assay Performance**

Confocal imaging of labeled cell lines demonstrated bright, punctate fluorescence predominantly localized at the cell membrane and cytoplasm, confirming effective nanoparticle binding and internalization, with signal intensity closely correlating with known biomarker expression levels. Magnetic nanoparticles enabled rapid and efficient magnetic separation of target cells and biomolecules from complex biological matrices, as evidenced by enhanced signal-to-noise ratios in downstream assays. In ex vivo tissue analysis, tumor sections exhibited distinct fluorescence signals co-localized with biomarker-rich regions, while adjacent normal tissue showed minimal background, highlighting the assay's high specificity and potential for clinical diagnostics.

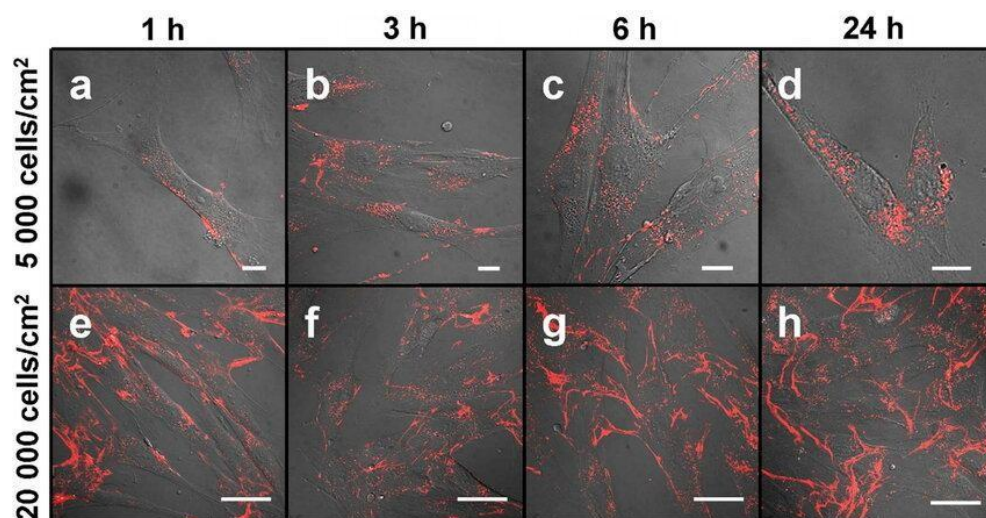


**Figure 7:** Confocal images show carboxylated QDs (red) in MSC cultures at low (5,000 cells/cm<sup>2</sup>; top) and high (20,000 cells/cm<sup>2</sup>; bottom) densities. At low density, QDs are intracellular; at high density, they deposit on cytoplasmic processes. Time points: 1, 3, 6, and 24 h post-exposure. Scale: 15  $\mu\text{m}$  (a–d), 50  $\mu\text{m}$  (e–h).

### 3.3 Comparative analysis

The dual-functional nanoparticle platform demonstrated significant advantages over conventional diagnostic methods such as ELISA and PCR. Unlike ELISA, which often requires longer incubation times and multiple washing steps, the nanoparticle-based assay enabled rapid detection typically under two hours while maintaining high sensitivity in the picomolar range. Compared to PCR, which is limited to nucleic acid targets and requires thermal cycling, this platform allowed direct detection of both protein and nucleic acid biomarkers without complex instrumentation. Furthermore, when benchmarked against commercially available nanoparticles lacking specific surface functionalization, the synthesized quantum dots and magnetic nanoparticles showed superior performance in terms of colloidal stability, biomarker binding efficiency, and signal intensity. The integration of magnetic separation with quantum dot fluorescence enhanced assay specificity and reduced background noise, particularly in complex biological samples. Overall, the system provided a streamlined, sensitive, and versatile diagnostic approach that surpasses many limitations of traditional single-modality assays.

### Conclusion:

In order to detect disease biomarkers early and sensitively, this study successfully created a hybrid nanodiagnostic platform that combines magnetic nanoparticles (MNPs) and quantum dots (QDs). With detection limits as low as 5 pM for protein biomarkers and 10 copies per

reaction for nucleic acid targets, the platform showed remarkable performance, attaining high specificity and sensitivity. The limitations of traditional techniques like ELISA and PCR were overcome by the quick, multiplexed detection made possible by the synergistic combination of magnetic enrichment and fluorescent amplification. The successful functionalization and characterization of QDs and MNPs, their biocompatibility in biological models, and their ability to target biomarkers specifically in both in vitro and ex vivo settings are important innovations. The platform is a promising tool for early disease diagnosis because of its dual-mode detection capability, which enhanced signal-to-noise ratios and offered real-time monitoring potential. Future studies continue to address issues like long-term stability, scalability, and clinical validation in spite of these developments. However, this study offers a solid basis for the development of next-generation diagnostic instruments, which have a great deal of promise to enhance patient outcomes, personalized medicine, and early disease detection. It will take more translational research and optimization to get this technology into clinical use.

#### References:

- [1] P. P., G. M., L. A., R. S., N. N., and E. E.P., “Quantum dots hold promise for early cancer imaging and detection,” *Int. J. Cancer*, vol. 131, no. 3, pp. 519–528, 2012, [Online]. Available: <http://www.embase.com/search/results?subaction=viewrecord&from=export&id=L51940547%0Ahttp://dx.doi.org/10.1002/ijc.27528>
- [2] P. Malik, S. Gulia, and R. Kakkar, “Quantum dots for diagnosis of cancers,” *Adv. Mater. Lett.*, vol. 4, no. 11, pp. 811–822, 2013, doi: 10.5185/amlett.2013.3437.
- [3] R. Mohammadi *et al.*, “Fluorescence sensing and imaging with carbon-based quantum dots for early diagnosis of cancer: A review,” *J. Pharm. Biomed. Anal.*, vol. 212, 2022, doi: 10.1016/j.jpba.2022.114628.
- [4] E. Ito, K. Iha, T. Yoshimura, K. Nakaishi, and S. Watabe, “Early diagnosis with ultrasensitive ELISA,” *Adv. Clin. Chem.*, vol. 101, pp. 121–133, 2021, doi: 10.1016/bs.acc.2020.06.002.
- [5] P. B. Jahrling, B. S. Niklasson, and J. B. McCormick, “Early Diagnosis of Human Lassa Fever By Elisa Detection of Antigen and Antibody,” *Lancet*, vol. 325, no. 8423, pp. 250–252, 1985, doi: 10.1016/S0140-6736(85)91029-3.
- [6] K. Iha *et al.*, “Ultrasensitive ELISA developed for diagnosis,” *Diagnostics*, vol. 9, no. 3, 2019, doi: 10.3390/diagnostics9030078.
- [7] Y. E. Choi, J. W. Kwak, and J. W. Park, “Nanotechnology for early cancer detection,” *Sensors*,

vol. 10, no. 1, pp. 428–455, 2010, doi: 10.3390/s100100428.

- [8] A. Tufani, A. Qureshi, and J. H. Niazi, “Iron oxide nanoparticles based magnetic luminescent quantum dots (MQDs) synthesis and biomedical/biological applications: A review,” *Mater. Sci. Eng. C*, vol. 118, 2021, doi: 10.1016/j.msec.2020.111545.
- [9] R. Koole, W. J. M. Mulder, M. M. Van Schooneveld, G. J. Strijkers, A. Meijerink, and K. Nicolay, “Magnetic quantum dots for multimodal imaging,” *Wiley Interdiscip. Rev. Nanomedicine Nanobiotechnology*, vol. 1, no. 5, pp. 475–491, 2009, doi: 10.1002/wnan.14.
- [10] R. Katwal, “A review: Properties and diverse applications of smart magnetic quantum dots,” *Nano-Structures and Nano-Objects*, vol. 35, 2023, doi: 10.1016/j.nanoso.2023.101001.
- [11] A. O. Govorov, “Optical and electronic properties of quantum dots with magnetic impurities,” *Comptes Rendus Phys.*, vol. 9, no. 8, pp. 857–873, 2008, doi: 10.1016/j.crhy.2008.10.007.
- [12] F. Rahimi, T. Ghaffary, Y. Naimi, and H. Khajehazad, “Effect of magnetic field on energy states and optical properties of quantum dots and quantum antidots,” *Opt. Quantum Electron.*, vol. 53, no. 1, 2021, doi: 10.1007/s11082-020-02695-w.